

# Searches for Beyond Standard Model Higgs bosons at the Tevatron

F. COUDERC

*CEA-Saclay/Irfu/SPP,*

*91191 Gif-Sur-Yvette Cedex, France*

This paper presents recent searches for minimal supersymmetric standard model (MSSM) Higgs bosons in  $p\bar{p}$  collisions at  $\sqrt{s} = 1.96$  TeV. These results have been obtained by the D0 and CDF experiments. We show analyses with up to  $7.3 \text{ fb}^{-1}$  of integrated luminosity. They probe a significant portion of the MSSM parameter space, being able to exclude  $\tan\beta > 25$  for low mass Higgs bosons  $m_A < 170$  GeV. We also report for Fermiophobic (FP) Higgs bosons searches in the  $\gamma\gamma$ , WW channels and their combination, which excludes FP Higgs bosons with masses  $m_{h_{FP}} < 119$  GeV.

## 1 MSSM Higgs bosons searches

While in the standard model (SM) only one Higgs boson doublet breaks the  $SU(2)$  symmetry, there are two Higgs boson doublets in the minimal supersymmetric standard model (MSSM)<sup>1</sup>. This leads to five physical Higgs bosons remaining after electroweak symmetry breaking; three neutrals:  $h$ ,  $H$ , and  $A$ , collectively denoted as  $\phi$ , and two charged,  $H^\pm$ . At the tree level, the mass spectrum of the Higgs bosons is determined by two parameters conventionally chosen to be  $\tan\beta$ , the ratio of the two Higgs doublet vacuum expectation values, and  $M_A$ , the mass of the pseudoscalar Higgs boson  $A$ . Although  $\tan\beta$  is a free parameter in the MSSM, large values ( $\tan\beta \gtrsim 20$ ) are preferred. The top quark to bottom quark mass ratio suggests  $\tan\beta \approx 35^2$ , and the observed density of dark matter also points towards high  $\tan\beta$  values<sup>3</sup>. In this large  $\tan\beta$  case, two of the neutral Higgs bosons ( $A$  and  $h$  or  $H$ ) are approximately degenerate in mass. They share similar couplings to quarks, enhanced by  $\tan\beta$  compared to the SM couplings for down-type fermions. The consequences of this enhanced coupling are first, that the main Higgs boson decay modes are  $\phi \rightarrow b\bar{b}$  and  $\phi \rightarrow \tau\tau$  with  $\mathcal{B}(\phi \rightarrow b\bar{b}) \approx 90\%$  and  $\mathcal{B}(\phi \rightarrow \tau\tau) \approx 10\%$ , respectively, and then, that their production in association with  $b$  quarks is enhanced by approximately  $\tan^2\beta$  compared to the SM.

Experiments at the CERN  $e^+e^-$  Collider (LEP) excluded MSSM Higgs boson masses below  $93 \text{ GeV}/c^2$ <sup>4</sup>. More recently, LHC experiments have also set stringent constraints on MSSM Higgs bosons properties<sup>5,6</sup>. We present here recent searches from the D0 and CDF experiments which extend the exclusion to higher masses for high  $\tan\beta$ . These experiments exploit the two Higgs boson decay modes  $\phi \rightarrow \tau\tau$  and  $\phi \rightarrow b\bar{b}$  to perform several searches with different sensitivity and backgrounds, the  $\phi \rightarrow b\bar{b}$  searches are nevertheless more sensitive to radiative corrections, hence to the MSSM parameters.

### 1.1 Inclusive searches in the di-tau channels

Both D0 and CDF experiments exploits the different  $\tau$  lepton decay modes:  $\tau \rightarrow \mu\nu_\mu\nu_\tau$  ( $\tau_\mu$ ),  $\tau \rightarrow e\nu_e\nu_\tau$  ( $\tau_e$ ) and hadronic  $\tau$  decays ( $\tau_h$ ) to do the search in different sub-channels:  $\tau_\mu\tau_h$ ,  $\tau_e\tau_h$ , and  $\tau_\mu\tau_e$ . The different analyses follow a similar strategy requiring exactly two oppositely

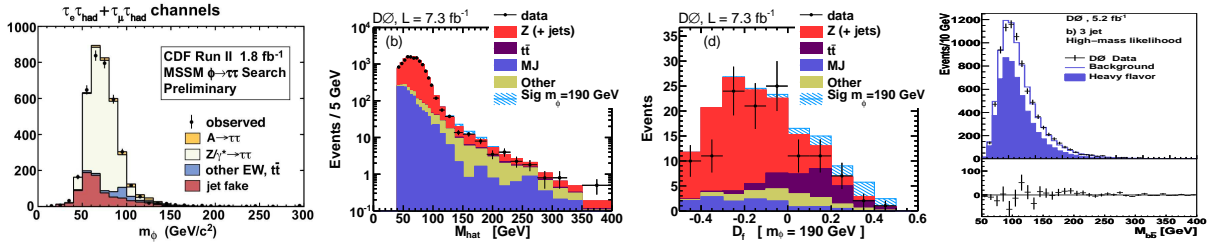


Figure 1: Left  $M_{vis}$  distribution at CDF in the combined  $\tau_e\tau_h + \tau_\mu\tau_h$  channel. Middle left:  $M_{vis}$  distribution at D0 in the  $\tau_\mu\tau_h$  channel. Middle right: Invariant mass of the best Higgs jet-pair at D0, background is fitted assuming no Higgs signal. Right:  $\mathcal{D}_f$  discriminant in  $b\tau_\mu\tau_h$  analysis for a Higgs boson mass of  $190 \text{ GeV}/c^2$ .

charged well identified leptons. In addition  $\mu$  and  $e$  must be isolated while  $\tau_h$  are required to be  $\tau_h$ -tagged. CDF searches employ  $\mathcal{L} = 1.8 \text{ fb}^{-1}$  of integrated luminosity<sup>9</sup>. D0 results<sup>10</sup> are based on  $\mathcal{L} = 7.3 \text{ fb}^{-1}$  but limited to the most sensitive channel  $\phi \rightarrow \tau_\mu\tau_h$ .

A set of cuts are imposed to suppress multijets (MJ),  $W$ +jets and,  $t\bar{t}$  backgrounds, the  $Z \rightarrow \tau\tau$  background being irreducible. Both experiments search for an excess in the  $M_{vis} = \sqrt{(p_{\tau\tau} + \not{p}_T)^2}$  distribution, where  $p_{\tau\tau}$  with  $\not{p}_T \equiv (\not{E}_T, \not{E}_x, \not{E}_y, 0)$ .  $M_{vis}$  distributions are shown on Fig. 1 for D0 and CDF experiments.

For both experiments no excess of data over expected background is observed. They both proceed to set model independent limits on  $\sigma(\phi \rightarrow \tau\tau) \times \mathcal{B}(\phi \rightarrow \tau\tau)$  as a function of the Higgs boson mass (assuming its natural width is negligible compared to the experimental resolution) and translate these constraints in different MSSM scenarii.

### 1.2 $b\phi \rightarrow b\bar{b}$ searches

An inclusive search  $\phi \rightarrow b\bar{b}$  is extremely difficult due to the abundant MJ background. Therefore, both experiments focus on the  $b\bar{b}$  final state where an additional  $b$  quark in the acceptance greatly reduces the MJ background. They require three  $b$ -tagged jets in the final selection. The MJ background dominates the sample and is modeled from a data-driven method. Both D0 and CDF search for a peak in the the Higgs jet-pair invariant mass distribution. The Higgs jet-pair is selected at D0 using a likelihood ( $\mathcal{LH}$ ) method while CDF selects the two leading jets. The selected jet-pair invariant mass distribution is modelled by using the MJ sample with exactly two  $b$ -tagged jets corrected for the presence of a third  $b$ -tagged jet. In both experiment, the composition of the signal sample is determined from a fit to data. See Fig. 1 for an example of the selected di-jet pair invariant mass at D0.

The analysis is performed with an integrated luminosity of  $2.6 \text{ fb}^{-1}$  by CDF<sup>11</sup> and  $5.2 \text{ fb}^{-1}$  at D0<sup>12</sup>. Both experiments does not observe any significant excess of data over the predicted background and set limit on the  $\sigma(bg \rightarrow b\phi) \times \mathcal{B}(\phi \rightarrow b\bar{b})$ . Limits on the different MSSM scenarii are also derived (taking into account the Higgs natural width).

### 1.3 $b\phi \rightarrow b\tau\tau$ searches

This channel is studied for by the D0 experiment in two different final states:  $b\tau_e\tau_h$  and  $b\tau_\mu\tau_h$ . The former<sup>13</sup> uses an integrated luminosity of  $3.7 \text{ fb}^{-1}$  while the latter<sup>14</sup> analyses  $7.3 \text{ fb}^{-1}$ .

The dominant backgrounds are coming from  $Z \rightarrow \tau\tau$ ,  $W$ +jets, MJ and  $t\bar{t}$ . The two analysis employs a similar strategy. The  $W$ +jets background is efficiently suppressed by a cut on the transverse mass formed by the  $\ell \equiv \mu/e$  and the  $\not{E}_T$ . Then, they developed multivariate discriminants against the main backgrounds, *i.e.* MJ and  $t\bar{t}$ , and combined them in a final discriminant  $\mathcal{D}_f$  which is used to perform for the search for a potential signal. In the case of the  $b\tau_\mu\tau_h$  analysis,  $b$ -tagging information are also included in  $\mathcal{D}_f$ . For this channel, the  $Z$  background is

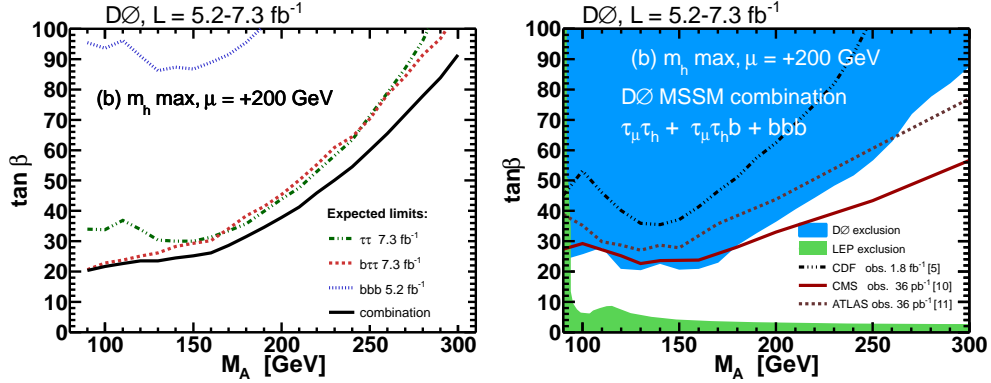


Figure 2: Left : Expected constraints in the  $(\tan\beta, M_A)$  plane from the D0 MSSM combination in the  $m_h$ -max scenario. Right: Observed constraints in the  $(\tan\beta, M_A)$  plane in the MSSM  $m_h$ -max scenario ( $\mu < 0$ ) from the D0 MSSM combination.

constrained from data using a  $Z \rightarrow \mu\mu$  control sample. Such a  $\mathcal{D}_f$  discriminant distribution is presented on Fig. 1 for the  $b\tau_\mu\tau_h$  channel.

No excess of data over predicted background is observed and limits are placed on  $\sigma(bg \rightarrow b\phi) \times \mathcal{B}(\phi \rightarrow \tau\tau)$ , and subsequently converted into constraints on the MSSM benchmark scenarii.

#### 1.4 D0 MSSM combination and conclusion

The D0 collaboration combined the three channels:  $\tau\tau$ ,  $b\tau\tau$  and  $b\bar{b}b$  to increase further the MSSM Higgs boson search sensitivity<sup>10</sup>. The expected constraints for each channels as well as the expected combined sensitivity are shown on Fig. 2 for the  $m_h$ -max MSSM scenario<sup>15</sup> with  $\mu > 0$ . The D0 collaboration does not observe any significant excess over the expected background and places constraint in the  $(\tan\beta, M_A)$  plane, taking into account the Higgs natural width. Examples are given on Fig. 2

D0 and CDF have actively searched for MSSM Higgs bosons. We presented here results with up to  $7.3 \text{ fb}^{-1}$  of integrated luminosity. In the absence of excess of data over expected background from SM processes, we set limits, strongly constraining the MSSM parameter space. We reach sensitivities down to  $\tan\beta \approx 20$  for low mass MSSM Higgs bosons.

## 2 Fermiophobic Higgs searches

In several beyond the standard model scenarii, the Higgs couplings to fermions are reduced. We study the extreme case where these couplings are cancelled. In this case, the Higgs production is restrained to vector-boson fusion (VBF) and vector-boson associated production (VH) while the  $\mathcal{B}(h_{FP} \rightarrow \gamma\gamma)$  is increased. Therefore the  $h_{FP} \rightarrow \gamma\gamma$  is enhanced by an order of magnitude compared to the SM which makes this final state the most promising channel at low mass to discover such a Higgs boson. The  $VH \rightarrow VWW^*$  is also very important at higher masses. Both collaboration uses the full Tevatron integrated luminosity ( $L \approx 10 \text{ fb}^{-1}$ ) to study the  $\gamma\gamma$  final state.

The search strategy uses the peculiar kinematic of this boosted production to optimize the sensitivity compared to the SM case. The CDF collaboration splits the sample into different categories depending on the diphoton mass resolution and on the transverse momentum of the diphoton pair while the D0 collaboration uses the same information combined with the invariant diphoton mass in a multivariate discriminant. The  $m_{\gamma\gamma}$  distribution in the most sensitive CDF channel and the D0 discriminant for  $m_{h_{FP}} = 120 \text{ GeV}$  are shown on Fig. 3 . The SM background is mainly coming from prompt di-photon production but also from  $\gamma$ +jets

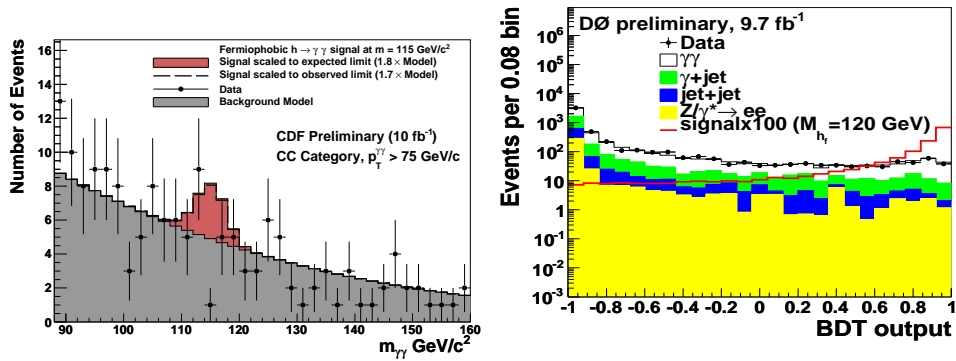


Figure 3: Left : CDF  $m_{\gamma\gamma}$  invariant mass for 2 isolated photons in the electromagnetic calorimeter barrel with  $p_T[\gamma\gamma] > 75 \text{ GeV}$ . Right: D0 final discriminant for  $m_{h_{FP}} = 120 \text{ GeV}$ .

production. It is estimated with a sliding window technique at CDF and a combination of a data-driven method (for  $\gamma$ +jets) and MC at D0. Both collaborations have similar sensitivity and none of them observe any significant excess over the expected background. Assuming the SM cross sections for VBF and VH productions, they set limits at:  $m_{h_{FP}} > 114 \text{ GeV}$  (CDF<sup>17</sup>) and  $m_{h_{FP}} > 111 \text{ GeV}$  (D0<sup>16</sup>).

The CDF collaboration has also combined this search in the  $\gamma\gamma$  final state with searches in  $WW$  and  $WWW^*$  channels which are also enhanced in FP models. They reach an expected sensitivity of  $m_{h_{FP}} > 119 \text{ GeV}$  while the observed limit is:  $m_{h_{FP}} > 115 \text{ GeV}$ .

## References

1. H. P. Nilles, Phys. Rep. **110**, 1 (1984); H. E. Haber and G. L. Kane, Phys. Rep. **117**, 75 (1985).
2. B. Ananthanarayan, G. Lazarides, and Q. Shafi, Phys. Rev. D **44**, 1613 (1991).
3. V. Barger and C. Kao, Phys. Lett. B **518**, 117 (2001).
4. S. Schael *et al.* (ALEPH, DELPHI, L3, and OPAL Collaborations), Eur. Phys. J. C **47**, 547 (2006).
5. S. Chatrchyan *et al.* (CMS Collaboration), Phys. Rev. Lett. **106**, 231801 (2011).
6. G. Aad *et al.* (ATLAS Collaboration), Phys. Lett. B **705**, 174 (2011).
7. V. M. Abazov *et al.* (D0 Collaboration), Phys. Lett. B **670**, 292 (2009).
8. A. Abulencia *et al.* (CDF Collaboration), Phys. Rev. Lett. **96**, 011802 (2006); D. E. Acosta *et al.* (CDF Collaboration), Phys. Rev. Lett. **95**, 131801 (2005).
9. T. Aaltonen *et al.*, (CDF Collaboration), Phys. Rev. Lett. **103**, 201801 (2009).
10. V. M. Abazov *et al.* (D0 Collaboration), Phys. Lett. B **710**, 569 (2012).
11. T. Aaltonen *et al.*, (CDF Collaboration), arXiv: 1106.4782, submitted to PRD.
12. V. M. Abazov *et al.* (D0 Collaboration), Phys. Lett. B **698**, 97 (2011).
13. V. M. Abazov *et al.* (D0 Collaboration), D0 Notes 5974-CONF.
14. V. M. Abazov *et al.* (D0 Collaboration), Phys. Rev. Lett. **107**, 121801 (2011).
15. M. Carena, S. Heinemeyer, C. E. M. Wagner, and G. Weiglein, Eur. Phys. J. C **45**, 797 (2006).
16. D0 Collaboration, Conference Note D0 Note 6297-CONF
17. CDF Collaboration, Conference Note CDF-10731